Numerical Simulations of the Interactive Coupling of Coastal Upwelling and Sea Breeze

Hsiao-ming Hsu
National Center for Atmospheric Research
P.O. Box 3000
Boulder CO, 80307

Abstract

To study mutual air-sea interaction in mesoscale, an atmosphere model and an ocean model have been coupled into a single system. The interaction between sea breeze and coastal upwelling appear in the numerical results from the fully coupled experiment, and the coupling produces negative feedback in an idealized situation. Comparing results with limited observations, there is good agreement in both diurnal and inertial signals.

1. Introduction

The importance of the interplay between atmosphere and ocean in large-scale air-sea interactions has been realized in analyzing both observed data and model results in recent climate studies. Similar interplay may also exist in smaller scales and should be explored because the impact of such smaller-scale air-sea interactions can be more direct and immediate than that of large-scale interactions. Over coastal regions, our life has been affected by both atmosphere and ocean, and their variabilities. A number of important and interesting phenomena are identified, such as storm surge, coastal upwelling, sea-land breeze, coastal frontogenesis and cyclongenesis, tropical cyclongenesis and cyclones, among others. Both coastal upwelling and sea-land breeze have appeared over some mid-latitude coastal regions, and their interaction can be mutual.

The coastal upwelling is induced by the along-shore wind stress to push the surface coastal water offshore due to the Ekman transport effect. The sub-surface water is lifted up because of the mass continuity, and it is colder and/or more salty than the surface water. On the other hand, in the atmosphere over coastal regions, the sea breeze is generated by the thermal contrast between land and sea surfaces. The thermal contrast is a consequence of much larger diurnal variation in the surface temperature over land than that over water. Low-level onshore flow during the day and offshore flow during the night are induced by such thermal contrast.

With upwelling, the coastal surface water becomes colder than one without upwelling. Thus, the thermal contrast between land and sea surfaces during the day becomes greater than the contrast without upwelling. However, the contrast during the night becomes less. Even if we assume the land-surface diurnal variation is symmetric between day and night, the thermal contrast is asymmetric due to the upwelling. The synoptic-scale flow, which supports the along-shore wind stress for upwelling, can further complicate the sea-land breeze circulation. It is interesting to understand how coastal water and atmosphere interact mutually.

Although both coastal upwelling and sea breeze are well known in oceanography and meteorology respectively, there never have been comprehensive and coordinated field program to focus the mutual coupling between them. Limited observations in the lower atmosphere, in addition to the well-planned oceanic observations during the Coastal Ocean Dynamic Experiment (CODE) showed some indications of such coupling. In Figure 1a, the kinetic energy spectra of wind at sensor level showed clearly the diurnal period of surface wind, and diurnal signal tended to be largest near the coast (Beardsley et al., 1987).

Winant et al. (1987) showed that such distinct frequency was also observed in the spectra of the alongshelf component of the wind stress (Figure 1b), and that the diurnal frequency variability appeared in both cross-shelf and alongshelf components of the current, in addition to a secondary peak of the inertial oscillation (Figure 1c). Therefore, the mutual coupling of coastal upwelling and sea breeze was postulated.

Clancy et al. (1979) made the first attempt to study the mutual interaction between sea-land breeze and coastal upwelling by coupling their four-layer atmosphere model to their two-layer ocean model through momentum and heat flux exchanges. They found that the air-sea feedback loop from the sea breeze process to the coastal upwelling process is exceedingly weak, although the sea breeze affected the upwelling and the upwelling affected the sea breeze. Later, Mizzi and Pielke (1984) studied the effect of the sea surface temperature pattern produced by an ocean model on the sea-land breeze circulation with their mesoscale numerical model. However, their atmosphere and ocean models were not mutually coupled. More recently, Chao (1992) developed a coupled atmosphere-ocean model system to study the interaction between atmospheric cold front and the Gulf Stream circulations. His dry two-dimensional numerical experiments suggested that atmosphere and ocean are mutually interactive and that the atmospheric influence on the coastal ocean is stronger than the the oceanic influence on the atmosphere.

To understand mutual interactions between ocean and atmosphere in mesoscale, it is beneficial to develop a numerical modeling system which couples an atmosphere model and an ocean model for three-dimensional mesoscale studies. Both models should have state-of-the-art parameterizations of subgrid-scale physics. The coupled system can be used not only for idealized numerical experiments but also for some real case studies. By performing different idealized simulations, possible regimes in which coupling may be possible can be established. Such information is invaluable for the planning of field experiments in the future. To further our understanding in coupled phenomena and to increase our confidence in numerical modeling, numerical experiments can be carried out for some realistic cases for special field programs. Limited available observational data sets can be utilized to verify numerical results, and further numerical results can help to interpret observed data.

To simulate realistic interactive coupling of coastal upwelling and sea breeze, it is important to parameterize the mechanisms of transferring momentum, heat, and water substance/moisture across the water surface accurately, because these mechanisms control the coupling between two fluids. These subgridscale turbulent transfers in the upper ocean and lower atmosphere determine dynamic and thermodynamic structures in both fluids. Not only the coupling mechanisms should be accurately represented, but also the physical processes in the lower atmosphere and upper ocean should be correctly parameterized. The sophistications of the physical parameterizations primarily depend on the scales of the scientific problems and our current understanding of the subgridscale processes.

In this paper, the mutual interaction between the coastal upwelling and sea breeze is demonstrated in the simplest hypothetical situation by turning off several physical processes in the models, such as precipitation, planetary boundary layer (PBL), and surface energy and moisture budgets. A simple coupled system is created so that the upper ocean circulation is driven by the horizontal variability of the wind stress, and that the lower atmosphere circulation is forced by the inhomogeneity of the surface temperature patterns. Two primitive-equation numerical models for atmosphere and ocean are included in the coupled system, and the simplest interactive mechanisms are also formulated and implemented. Some model results will be discussed.

2. The Models and the Coupling

Scientifically, the numerical results from this simplest coupling will indicate that the mutual interaction between coastal upwelling and sea breeze can be realized under certain conditions. Even though some of the parameters utilized in the simulations are idealized, the results are interesting and encouraging. Technically, a primitive-equation atmosphere model (Hsu, 1987) and a primitive-equation ocean model with an active surface mixed-layer (Haidvogel, et al., 1991, and Price, et al., 1986) have been coupled together successfully. Further details and tests of the ocean

model can be found in Hermann and Hsu (1993). Even though both models are three–dimensional, for this demonstration of feasibility in coupling study, it is assumed that circulations in the along–channel direction are invariant. Before describing some model results, some coupling mechanisms are briefed as follows.

The individual models for atmosphere and ocean have been modified and included in a single model system. The atmosphere component is forced by a combination of the horizontal distributions of the ground surface temperature and the ocean surface temperature. The ground surface is assumed to experience a simple diurnal variation (sine function in time only), while the ocean surface temperature is a consequence of the ocean circulation beneath the ocean surface. The heat flux from the surface is calculated by a constant diffusivity formulae. Because the ocean model now only has the density as a dependent variable to represent the combined effect of temperature and salinity, the ocean surface temperature is obtained by a simple linear relationship between the density and the temperature.

On the other hand, the ocean component is driven by the wind stress at the ocean surface. The wind stress is computed from the wind velocity at a height of 10 m above the ocean surface based on the recent study of Hsu (1986). This formulation incorporates the contribution of both winds and waves through the parameterization of an aerodynamic roughness equation. The atmospheric circulations are mostly induced in the lower atmosphere and control the wind stress variations which drive the upper ocean. The primary oceanic circulations are generated in the upper ocean and determine the surface temperature distribution which provides the thermal contrast at the surface and forces the lower atmosphere.

In general, the internal responses of both atmosphere and ocean differ greatly, because of their intrinsic temporal and spatial scales. Different grid spacings and time steps usually cause difficulty in coupling an atmosphere model and an ocean model into a system. However, the coastal upwelling and sea breeze have close spatial scales, even though their temporal scales are somewhat different. The sea breeze basically is diurnal, while the upwelling extends to at least several days. Therefore, same horizontal grid spacing is utilized in the coupled system. The time step for the atmosphere model is at least an order of magnitude smaller than that for the ocean model. For example, the atmospheric component may be executed 10 times, while the ocean component may be carried out only once.

3. Numerical Results

To present the simplest coupling between the coastal upwelling and sea breeze, only the essential physics are retained in the coupled system. In the atmospheric model, both parameterizations of the precipitation processes and the ground surface energy and moisture budgets have been turned off. The parameterization of the turbulent transfers in the lower atmosphere has been replaced by a constant eddy exchange coefficient to represent the K–profiles computed by the parameterized PBL physics. In the ocean model, the surface thermal forcing has been inactive with the intention to demonstrate that the diurnal signatures in the ocean is a direct consequence of the atmospheric forcing through the wind stress, which is calculated from the 10–meter wind field.

Schematically, the two–dimensional coupled atmosphere and ocean system is presented in Figure 2. The shaded area is the land, and the numbers in the parentheses indicate the grid numbers. Initially, the model atmosphere is neutrally stratified below 2 km and uniformly stably stratified above, and the model ocean has a thermocline layer centered at a depth of 30 m. The Coriolis parameter is set to be $1. \times 10^{-4}$ s^{-1}. Several experiments were conducted for a five–day period.

a. Atmospheric circulations

First, a control experiment was executed using the coupled system under an initial uniform wind speed of 10 m s^{-1} along the channel, and the atmospheric thermal fields (Figure 3) show an asymmetric evolution of the narrow unstable columns associated with the sea breeze fronts. As the land surface experiences the daytime phase of the diurnal cycle, most of the ocean surface temperature remains constant, except a noticeable cooling at the left side of the channel. The cooling comes from the coastal upwelling, an oceanic response to the along–channel wind stress. The stable atmosphere above the initially

neutral PBL is also affected by the convection along the sea breeze front. The corresponding vertical velocity fields are shown in Figure 4. The updrafts due to the sea breeze convergence are distinct. The sea breeze fronts move inland at different speeds at opposite sides of the channel. The initial along-channel wind generates a cross-channel wind due to the Coriolis effect. At the right coast of the channel, the wind is onshore but is offshore at the left coast. This onshore wind helps the right sea breeze front to move inland much faster than the one on the other side of the channel.

In order to understand the effect of the upwelling cooling at the ocean surface on the atmospheric coastal circulation, a numerical experiment was conducted using only the atmosphere model. Otherwise, this experiment has the identical specifications to the control experiment. Figure 5 shows the daytime evolution of the vertical velocity fields. Comparing the results from the control experiment, the updraft along the left coast of the channel has not yet appeared at the 99th hour of the simulation (Figure 5a). On the other hand, there is a clearly defined updraft along the left coast in the control experiment (Figure 4a). This updraft is mainly supported by a stronger surface temperature contrast across the coast, because the coastal upwelling cooling enhances the cross-coast temperature gradient. Otherwise, the sea breeze circulations from both cases are quite similar. As will be seen later, the thermocline layer in the ocean has not completed its outcropping process at the end of the simulations (120 hours), and the ocean surface cooling along the upwelling coast has not yet reached its maximum yet. It is expected that the atmosphere response will increase after the thermocline layer is completely outcropped and moves off coast.

Temporal variations of the wind at the height of 10 m, where the wind information is used to compute the wind stress to drive the ocean circulation, are presented in Figure 6. The variations in the wind field are clearly diurnal, but horizontally they are not uniform (Figures 6a and 6b). Along-channel speed (U) is reduced significantly to about 5 m s^{-1} along the left coast because of the nature of the Ekman layer. This has strong implication to the coupled ocean circulation, which will be discussed later. The low-level sea breeze convergence along both coasts can be found in the cross-channel speed (V) field. Each sea breeze convergence on the left coast starts at the coast and propagates inland. On the other hand, significant convergence does appear immediately at the right coast until about 15 km inland. These low-level convergence zones coincide with the updrafts (Figure 6c). The cellular structure in each updraft band suggests periodic variation of the sea breeze front. The land surface temperature varies diurnally as specified, but over the ocean surface, cooling due to upwelling increases its strength and area as the thermocline layer gradually outcrops from the ocean depth (Figure 6d).

Without any ambient wind at the beginning of the numerical experiment, the coupled system is only driven by the diurnal heating/cooling over the land surface. Figure 7 shows the results from this simulation to compare with those from the control case (Figure 6). The asymmetric pattern of the numerical solution in the control case does not appear in the present solution. Symmetry and diurnal cycle are the prominent features in this case.

b. Oceanic circulations

In the control experiment, the atmosphere has an initial constant wind of 10 m s^{-1} in the along-channel direction. Even though the 10-m wind is modified by the parameterized PBL physics to an along-channel speed about 5 m s^{-1}, the initial thermocline layer centered at 30 m depth is pushed upward along the left coast and downward along the right coast. After 5 days of simulation, only half of the thermocline layer outcrops (Figure 8a). In the next experiment, the atmosphere model is decoupled, and the ocean is simply driven by a constant along-channel wind stress based on a wind speed of 10 m s^{-1}. The relationship between the wind stress and the 10-m wind is the same as the one used in the control experiment. The thermocline layer outcrops much faster (Figure 8b) than the one in the control case. This difference is caused by the different wind stress applied to the ocean surface. The wind stress in the ocean-alone experiment is a simple constant, but the fully coupled experiment has both diurnal and PBL effects, and comparatively, the latter is much weaker than the former. When the ambient wind in the atmosphere is turned off, the wind stress generated by the sea breeze alone is so weak that it cannot exert enough influence on the ocean to disturb the thermocline after 5 days of sim-

ulation (Figure 8c).

The time series of the upwelling for these cases (Figure 9) show that the ocean–alone experiment provides fastest upwelling (Figure 9b) and the coupled case without any ambient wind has essentially no upwelling (Figure 9c). The result from the control experiment (Figure 9a) shows not only that the sub–surface dense water upwells, but also has some oscillations. To further understand the nature of the oscillations in the model results, the time series of the surface currents from these three experiments are presented in Figure 10. The surface currents from the control experiment show a somewhat complicated oscillation pattern in both along– and cross–channel directions (Figures 10a and 10b). However, the ocean–alone experiment does not support any significant oscillation (Figures 10c and 10d), even though it has the strongest wind–stress forcing over a 5–day period. When the ambient wind is shut down in the coupled experiment, interestingly enough, the surface currents display organized oscillation patterns (Figures 10e and 10f).

In order to determine the property of the oscillations, a temporal spectral analysis is applied to the current data. For the control case, both diurnal cycle (period 5, 24 hours) and inertial cycle (period 7, 17 hours) clearly are dominant (Figure 11a and 11b). The diurnal cycle comes from the imposed diurnal variation at the land surface. The diurnal thermal contrast between the land and ocean surfaces induces the sea–land breeze. Such diurnal circulation signals become part of the 10–m wind field, and support the diurnal wind stress to force the ocean. The inertial cycle is the intrinsic frequency of the ocean when it is forced by a wind stress in the mid–latitude. For the ocean–alone case, the wind stress based on the wind speed of 10 m s^{-1} fails to produce the inertial cycle (Figures 11c and 11d), and the reason is not clear at this point. In the results from the coupled experiment without any ambient wind, the diurnal cycles appearing next to the coasts are the consequence of the effect of the pure sea–land breeze. Weak inertial periods also appear.

4. Discussion

As demonstrated in the results from numerical experiments, the atmosphere and ocean have mutual interaction in mesoscale. From the fully coupled experiment, the daytime sea breeze is enhanced by the increased thermal contrast across the left coast due to the upwelling cooling along the coast, while the upwelling of the thermocline layer is reduced by the modified wind stress affected by the diurnal sea–land breeze circulations. Without ambient wind, the model results suggest that the interaction between sea breeze and coastal upwelling is exceedingly weak. It will be interesting to learn the condition for the coupling even in this idealized situation to help in understanding the coupling processes better.

The reduction in the strength of the coastal upwelling in the fully coupled experiment indicates the coupling between the sea breeze and coastal upwelling is negative. This conclusion is in agreement with the earlier studies of Clancy et al. (1979) and Mizzi and Pielke (1984).

Most importantly, the oscillations observed in the model results are consistent with the observations made during the CODE periods. The diurnal frequency dominates but both diurnal and inertial signals are present in the ocean. Further quantitative comparison of model data from more realistic experiments using the fully coupled modeling system with the CODE data sets should reveal the additional details in coupling.

The current numerical modeling system employs a horizontal grid–spacing of 2.5 km. Further study should increase the horizontal resolution to obtain more accurate results. This leads to the improvement of the present atmosphere model from the hydrostatic calculation to the nonhydrostatic one. Moreover, the PBL parameterization may be simplified because this improvement will enable the model to directly resolve the PBL transfer mechanisms, at least to the large eddies. Also, the bulk mixing approach toward the boundary layer mixing in the present ocean model should be replaced by a turbulence–closure approach to reduce the small-scale fluctuations.

References

Beardsley, R.C., C.E. Dorman, C.A. Friehe, L.K. Rosenfeld, C. D. Winant, 1987: Local atmospheric forcing during the Coastal Ocean Dynamics Experiment. 1. A description of the marine bound-

ary layer and atmospheric conditions over a northern California upwelling region. *J. of Geophys. Res.*, **92**, 1467–1488.

Chao, S.-Y., 1992: An air-sea interaction model for cold–air outbreaks. *J. of Phys. Oceanogr.*, **22**, 821–842.

Clancy, M.R., J.D. Thompson and H.E. Hurlburt, 1979: A model of mesoscale air–sea interaction in a sea breeze–coastal upwelling regime. *Mon. Wea. Rev.*, **107**, 1476–1505.

Haidvogel, D.B., J.L. Wilkin and R.E. Young, 1991: A semi–spectral primitive equation ocean circulation model using vertical sigma and horizontal orthogonal curvilinear coordinates. *J. of Computat. Phys.*, **94**, 151–185.

Hermann, A.J., and B. Hsu, 1993: A vertical coordinate mapping technique for semispectral primitive equation models of ocean circulations. *J. of Atmos. Oceanic Technol.*, **10**, 381–396.

Hsu, H., 1987. Mesoscale lake–effect snowstorms in the vicinity of Lake Michigan: linear theory and numerical simulations. *J. of the Atmos. Sci.*, **44**, 1019–1040.

Hsu, S.A., 1986: A mechanism for the increase of wind stress (drag) coefficient with wind speed over water surfaces: A parametric model. *J. of Phys. Oceanogr.*, **16**, 144–150.

Mizzi, A.P. and R.A. Pielke, 1984: A numerical study of the mesoscale atmospheric circulation observed during a coastal upwelling event on 23 August 1972. Part I: Sensitivity studies. *Mon. Wea. Rev.*, **112**, 76–90.

Price J. F., R. A. Weller, and R. Pinkel, 1986. Diurnal cycling: Observations and models of the upper ocean response to diurnal heating, cooling, and wind mixing. *J. of Geophys. Res.*, **91**, 8411–8427.

Winant, C.D., R.C. Beardsley, R.E. Davis, 1987: Moored wind,temperature, and current observations made during Coastal Ocean Dynamics Experiments 1 and 2 over northern California continental shelf and upper slope. *J. of Geophys. Res.*, **92**, 1569–1604.

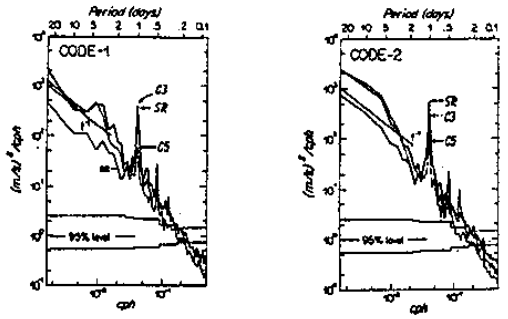

Fig. 1a Kinetic energy spectra of wind measured at sensor height at Sea Ranch, C3, and C5 during the CODE 1 and CODE 2 common analysis period. A 2–day cosine taper was applied to the ends of the time series before Fourier transforming and band averaging. The 95% confidence limits are shown. Lines with a slope of -1 have been added for reference. (After Beardsley et al., 1987)

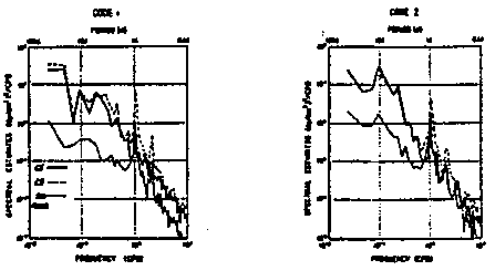

Fig. 1b Spectra of the alongshelf component of wind stress at Sea Ranch, C3, and C5 along the C line during CODE 1 and CODE 2. (After Winant et al., 1987)

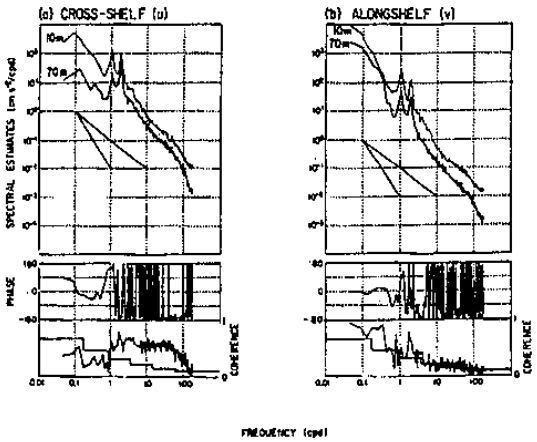

Fig. 1c Spectra, coherence and phase of (a) cross-shelf and (b) alongshelf components of currents observer 10 m beneath the surface (light line) and 70 m beneath the surface (heavy line) at C3 during the CODE 2 common period. Reference lines with -1 and -2 slope have been added to the current spectra. Note that spectra are plotted with different scales. The steplike line in the coherence plot is the value above which there is 95% probability the real coherence is not zero. The orientation of positive alongshelf flow is 317°N. (After Winant et al., 1987)

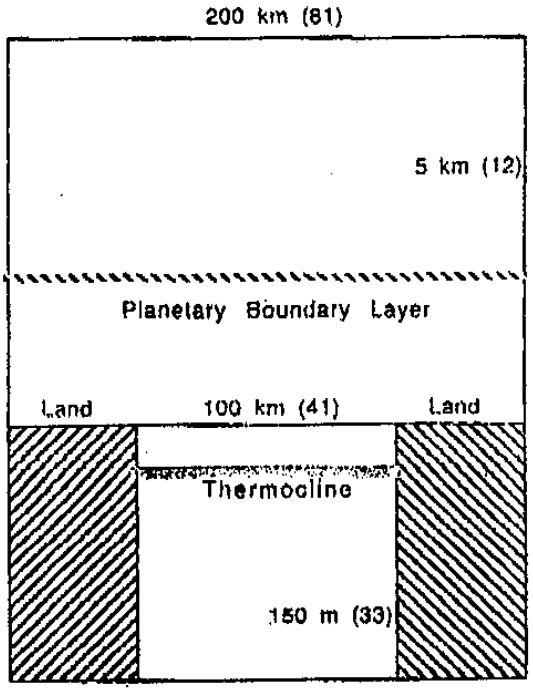

Fig. 2 Schematic representation of a coupled model for the sea-land breeze and coastal upwelling.

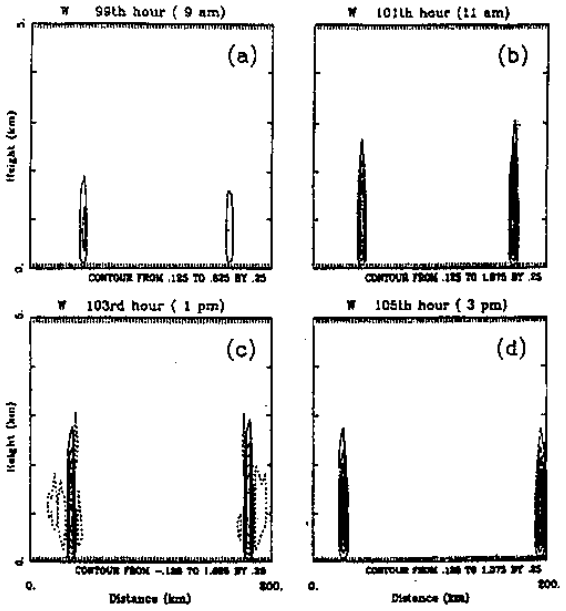

Fig. 4 Vertical cross-sections of vertical velocity (m s^{-1}) for the control experiment.

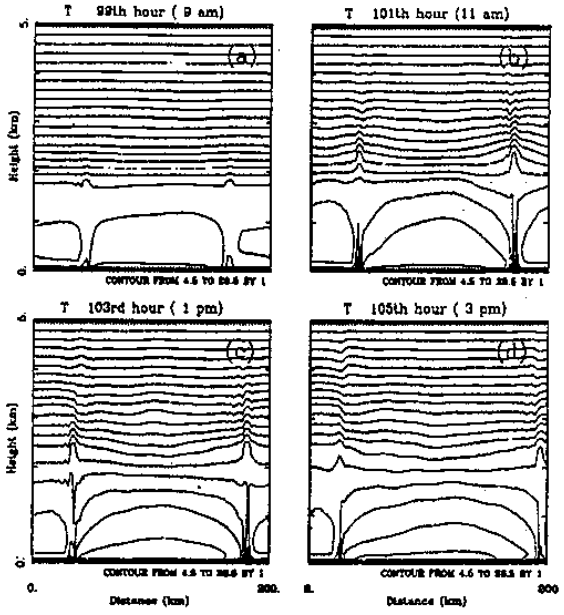

Fig. 3 Vertical cross-sections of potential temperature (°K + 273.16) for the control experiment.

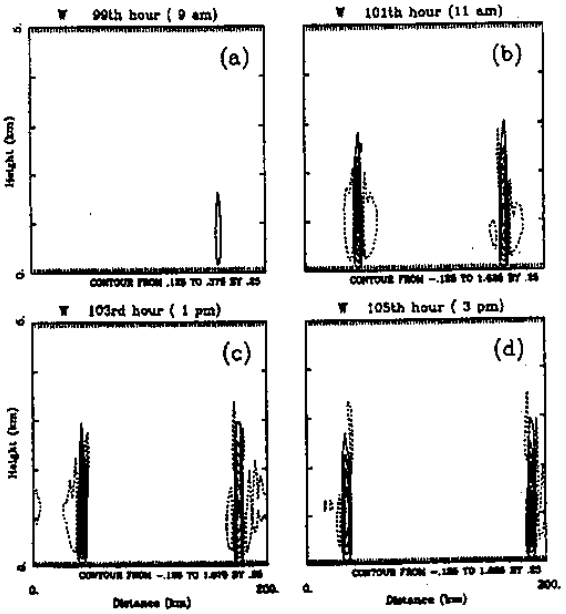

Fig. 5 Vertical cross-sections of vertical velocity (m s^{-1}) for the atmosphere-alone experiment with the ambient wind of 10 m s^{-1}.

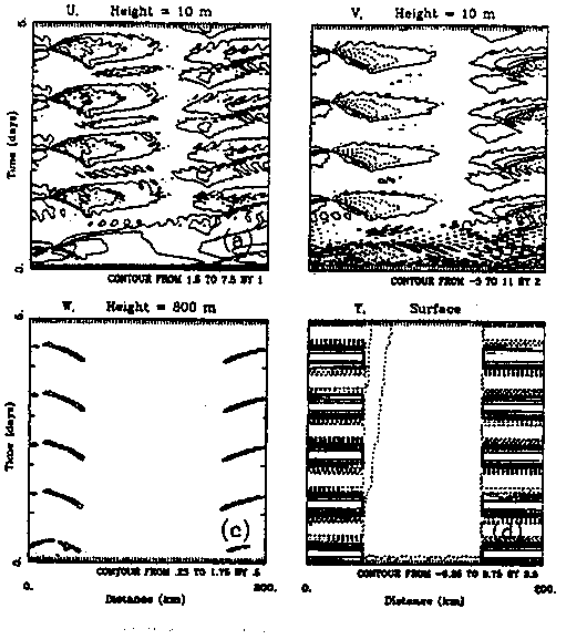

Fig. 6 Time series of U at 10 m, V at 10 m, W at 800 m and surface potential temperature across the model domain for the control experiment. Velocity in the unit of m s^{-1}, and potential temperature in the unit of °K + 273.16.

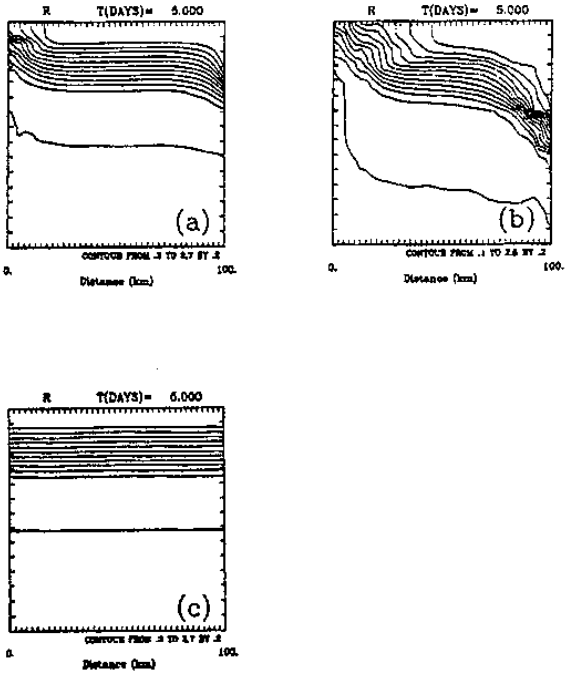

Fig. 8 Vertical cross-sections of density perturbation (σ) for the control experiment (a), the ocean-alone experiment with a wind stress based on the 10-m wind of 10 m s^{-1} (b), and the coupled experiment without any ambient wind (c).

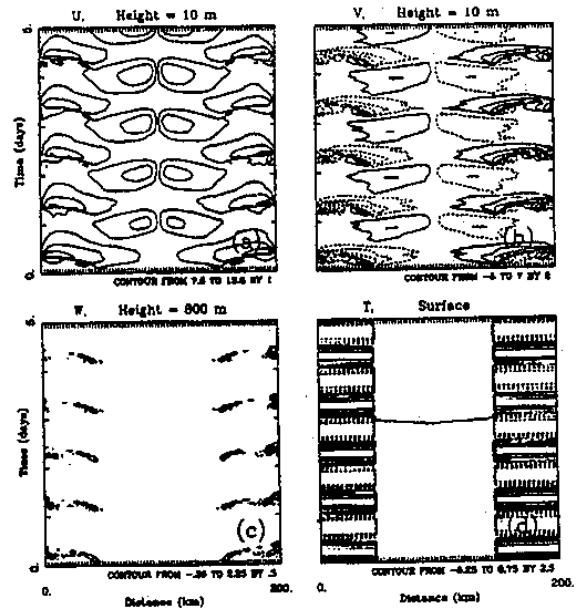

Fig. 7 Same as Fig. 6 except that this experiment without any ambient wind.

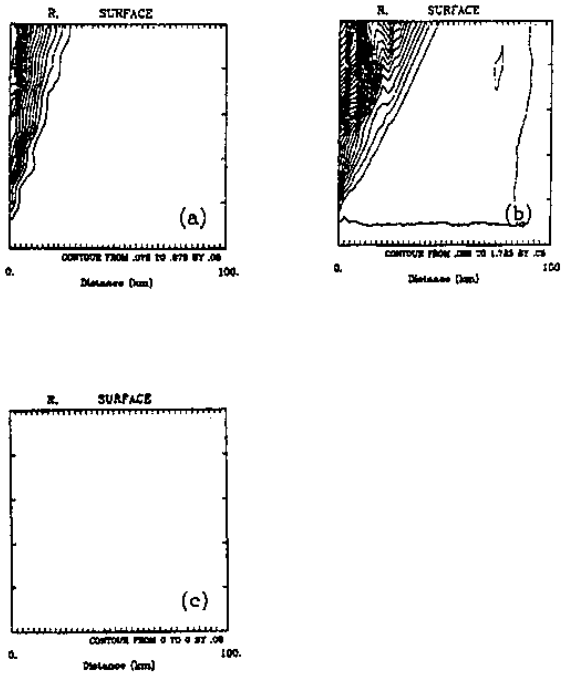

Fig. 9 Time series of surface density perturbation (σ) for the control experiment (a), the ocean-alone experiment with a wind stress based on the 10-m wind of 10 m s^{-1} (b), and the coupled experiment without any ambient wind (c).

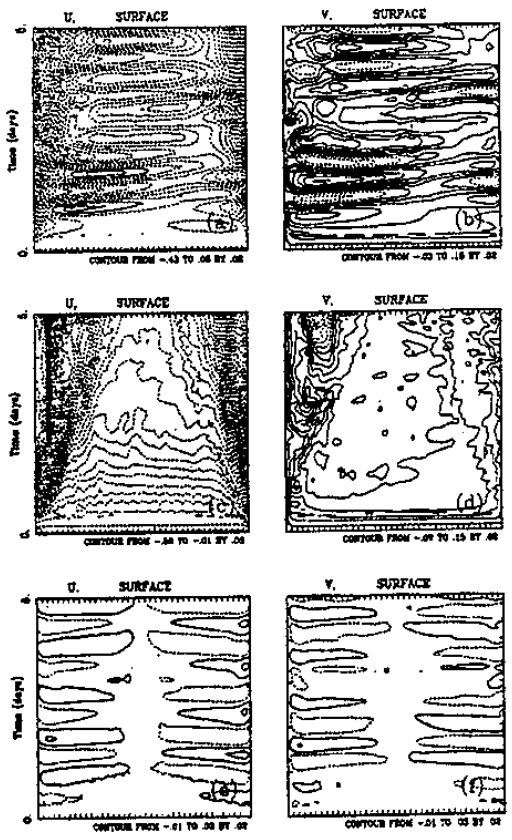

Fig. 10 Time series of surface currents (U and V) in the unit of m s^{-1} for the control experiment (a), the ocean–alone experiment with a wind stress based on the 10–m wind of 10 m s^{-1} (b), and the coupled experiment without any ambient wind (c).

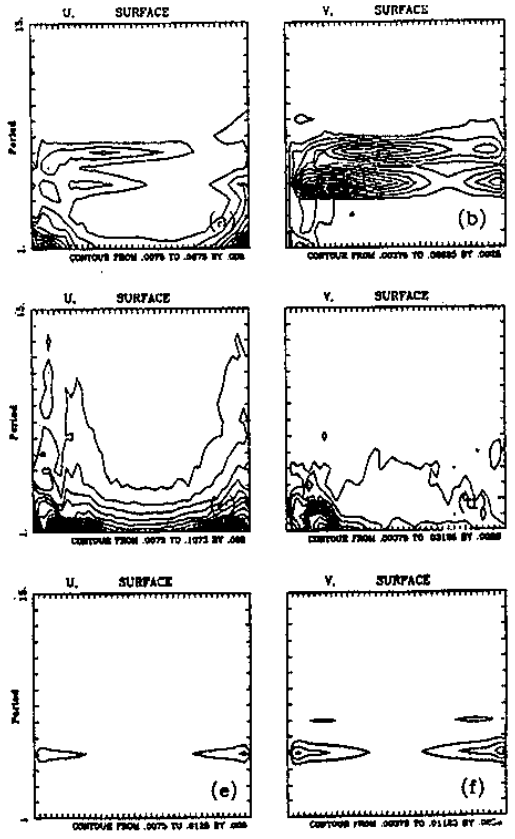

Fig. 11 Spectra of surface currents for the control experiment (a), the ocean–alone experiment with a wind stress based on the 10–m wind of 10 m s^{-1} (b), and the coupled experiment without any ambient wind (c).